BULLETIN OF THE POLISH ACADEMY OF SCIENCES
TECHNICAL SCIENCES, Vol. 68, No. 3, 2020
DOI: 10.24425/bpasts.2020.133383

Power supply with parallel reactive and distortion power compensation and tunable inductive filter – Part 1

M. GWÓŹDŹ, Ł. CIEPLIŃSKI*, and M. KRYSTKOWIAK

Poznan University of Technology, Faculty of Control, Robotics and Electrical Engineering, Piotrowo 3A, 60-965 Poznan, Poland

Abstract. The work presents a DC power supply with power factor correction (PFC). This device is also equipped with a parallel active filter function, which enables the possibility of compensation (minimization) of reactive and distortion power, generated by a group of loads, connected to the same power grid node. A passive filter with variable inductance applied at the input of the power supply allows for a significant improvement in quality of the system control (given specific criteria), as compared to the solution with a filter with fixed parameters. This is possible by increasing the dynamics of current changes at the power supply input (extending its "frequency response"). The paper presents the principle of operation as well as structures and models of the power supply control system and its power stage. Selected test results of the simulation model of the electric system with the power supply, in various operating conditions, are also presented.

Key words: distortion power, PFC, power supply, reactive power, tunable inductive filter.

1. Introduction

The negative impact of nonlinear loads on the operation of the power grid is widely known and confirmed by many studies, e.g. [1–3]. For example, widely used conventional solutions with rectifiers (diode and thyristor), as well as functionally simplified switched-mode power supplies, draw strongly distorted current, which results in their negative impact on the power grid. The most important of which are: increase in power losses, reduction of grid capacity, and generation of electromagnetic disturbances. One of their direct effects is the reduction of the lifetime of both the grid itself and the loads connected to it (including those that do not have a negative impact on its operation). So, in addition to the technical context, it should be considered in terms of a purely economic and even social (e.g. health) impact. Therefore, various types of "compensators"', mainly filters (passive and active), are used in the electrical systems as a preventive measure. The main task of these devices is appropriate matching of the current's shape at its input to the shape of a current drawn from the same power grid node by other loads. As a result of the compensation process, understood in this way, the total current drawn from the power grid node should have both a suitable shape and phase relation with a voltage in the power grid – depending on a compensation strategy, e.g. [4–7]. A main disadvantage of these devices is related to the fact that they have only one specialized function in the power system. Thus, the solutions of systems to improve energy quality, seen in the literature (and technology), do not perform certain tasks comprehensively. They focus, for example, on active parallel compensation, e.g. [8–14], (less often – serial) – without the possibility of supplying external loads – or perform such compensation in a limited range, e.g. only for reactive power.

In this work, the DC power supply with the ability of active compensation of a reactive and distortion power is proposed. Moreover, thanks to extending the "frequency response" of a power electronics current source, which is a part of the power supply, the quality of the compensation process is better, compared to most of the typical solutions of active filters.

The following sections of the paper are presented: the principle of operation of the power supply, the structure of both its power electronics and control section, the linear model of the controlled current source, the principle of operation of a tunable inductive filter, and investigation results of the simulation model of the electrical system with the power supply. The last part of the paper is devoted to the conclusions.

2. Principle of operation of power supply with tunable inductive filter

Higher current harmonics, flowing through the elements of the power grid, cause voltage drops on them $(\Delta U_{\mathrm{L},n})$, which are formally described by the following formula

$$\Delta U_{\mathrm{L},n} = I_{\mathrm{L},n} Z_{\mathrm{L},n}\,, \qquad n = 2,3,\ldots\,, \tag{1}$$

where: $I_{\mathrm{L},n}$ is RMS value of n-th current harmonic, $Z_{\mathrm{L},n}$ is resultant power grid impedance for n-th current harmonic.

As a consequence, voltage in a power grid can be strongly distorted, as illustrated in Fig. 1, which shows the exemplary waveforms of voltage and current in the "soft" power grid. The significantly nonlinear current, shown in this figure, is

*e-mail: lukasz.cieplinski@put.poznan.pl

Manuscript submitted 2019-10-28, revised 2020-01-12, initially accepted for publication 2020-02-06, published in June 2020

caused by a thyristor-based voltage regulator, loaded with a resistor.

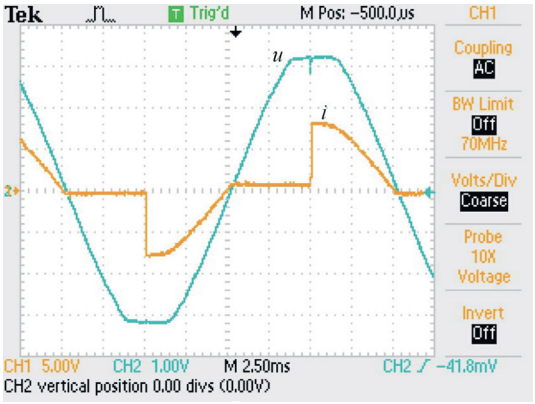

Fig. 1. Real waveforms of grid voltage and load current in a "soft" power grid

The general block diagram of the electrical system, including the proposed power supply, cooperating with nonlinear loads connected to the same power grid node, is shown in Fig. 2. The system (PS) with such topology is capable of fulfilling the role of a parallel active filter.

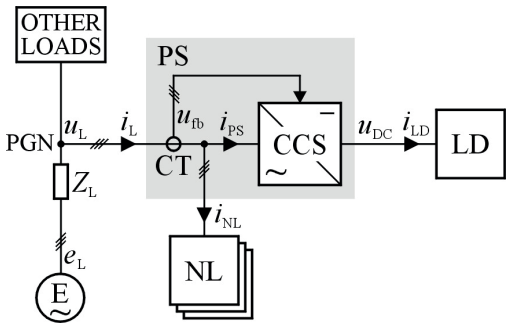

Fig. 2. Block diagram of the electrical system, including the power supply with compensation function

However, at the current stage of studies, it was assumed that the system is based on a 1-phase grid and the block denoted as "OTHER LOADS" is not present there.

Thus, the system consists of the following basic components:

- E – power source; *emf* is $e_L = E_L \sin(\omega_L t)$, where E_L and ω_L are, respectively, amplitude and frequency,
- PGN – power grid node (with an internal impedance of a power grid denoted as Z_L),
- PS – power supply which is the subject of research, consisting of a power electronics controlled current source (CCS) and current transducer (CT),
- NL – a group of nonlinear loads, i.e. other devices connected to the same power grid node as the power supply,
- LD –load of power supply.

The power theory introduced by Fryze was chosen for control of the power supply (i.e. its compensation function) [15]. According to this theory, the general aim of optimization of the power grid current (i_L) is minimization of its RMS value. It results, among others, in minimization of power losses, while an energy transfer from an energy source (E) to a load occurs. Therefore, the desired resultant current, drawn from the grid by the system, is described by the following formula

$$i_L = i_{NL} + i_{PS} = i_{ref,L} = I_{ref,L} \sin(\omega_L t), \tag{2}$$

where: i_{NL} is total current of the group of nonlinear loads, i_{PS} is power supply input current, and $I_{ref,L}$ is current amplitude.

Thus, the power supply generates distorted (in general) current at its input, which, when combined with the current of nonlinear loads, results in a sinusoidal (theoretically) current, drawn from a grid. This current is in-phase with the network voltage. As a result, the negative impact of nonlinear loads (i.e. NL block) on the power grid is eliminated, and in the real system it is minimized. The operation of the system as a whole is therefore consistent with the PFC function [16–22].

3. The structure of the input section of the power supply

The input circuit of the power supply consists of an H-type transistor bridge with an inductive filter (L-TI) at the input (Fig. 3). Both of these blocks form a power electronics controlled current source (CCS) [21–23]. The current source's task is not only to provide the required voltage in the DC circuit (u_{DC}) of the power supply, to which the main load (LD) is connected but also to actively compensate for phase shift and higher harmonics of current drawn by nonlinear loads (NL). The role of the filter is twofold – it increases the input impedance of the current source and minimizes the magnitude of the input current component associated with pulse modulation (here PWM) [21, 22].

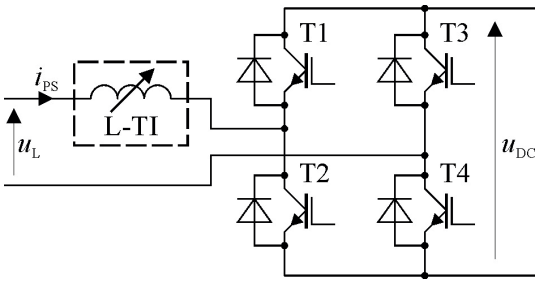

Fig. 3. Diagram of the input power electronics stage of the power supply

Taking into account the diagram shown in Fig. 3 and assuming that during the given half-periods of the mains voltage, appropriate pairs (i.e. T1–T4 or T3–T2) of the bridge switches are turned on, the source current waveform is described by the following general formula (however, not respecting: filter resistance, grid impedance as well as voltage drops at power devices in the converter)

$$i_{PS}(t) = \frac{1}{L_{TI}} \int \left[u_{DC}(t) - |u_L(t)| \right] \mathrm{d}t\,, \tag{3}$$

where: L_{TI} is filter's inductance at the current source input.

The ability of shaping the PS input current by the current source is mainly determined by a value of its bandwidth (BW), i.e. the "frequency response". Taking into account the linear model of a current source (analyzed in Section 6), BW is determined by the following formula [24]

$$BW = \frac{1}{2\pi I_{\mathrm{PS}}} SR, \tag{4}$$

where: I_{PS} is a magnitude of the input current of the CCS, and SR is a slew rate of this current [24].

With the assumptions made, the SR parameter results directly from the value of the first derivative of the source current waveform, and therefore

$$SR = \left. \frac{u_{\mathrm{DC}}(t) - |U_{\mathrm{L}} \sin(\omega_{\mathrm{L}} t)|}{L_{\mathrm{TI}}} \right|_{t=t_0}, \tag{5}$$

where: U_{L} is grid voltage amplitude.

The source current's slew rate depends on the instantaneous value of the grid voltage, reaching (in relation to the first half-period of voltage) its extreme values, described by the following formulas

$$SR_{\max} = \left. \frac{u_{\mathrm{DC}}(t_0)}{L_{\mathrm{TI}}} \right|_{t=t_0}, \tag{6}$$

$$SR_{\min} = \left. \frac{u_{\mathrm{DC}}(t_0) - U_{\mathrm{L}}}{L_{\mathrm{TI}}} \right|_{t=\frac{\pi}{2\omega_{\mathrm{L}}}}. \tag{7}$$

As it results from (6) and (7), the source has the narrowest bandwidth when the instantaneous value of the grid voltage reaches the maximum value, and the widest such value when the voltage in the power grid passes through zero. Considering that both the value of the network voltage and the voltage in the DC circuit of the power supply are imposed in advance, the only factor that can increase the dynamics of changes of the source current is the reduction of the filter inductance, which, however, results in an increase in the amplitude of the PWM carrier component in the input (grid) current.

Therefore, in order to increase the "frequency response" of the power source, it was proposed to use an inductive filter (in the form of a choke) with a variable inductance value. This solution allows a better approximation of a grid current shape to the "ideal" waveform, imposed by (2) – in a situation of high dynamics of current changes – in relation to a CCS with a constant inductance value of a filter. At the same time, in steady states, the magnitude of the pulse modulation carrier component in the power supply input current remains at a minimal level.

4. The principle of operation of a tunable inductive filter

For the implementation of the tunable inductive filter, the phenomenon of coupling of magnetic fluxes of two coils was used. As a result, their resulting magnetic flux can be amplified or reduced, which results in a change in equivalent inductance. In the basic version of the system, the value of the equivalent reactance (X_{TI}) of the filter, at the power source part (u_1), can reach two values – depending on the position of the S switch (Fig. 4).

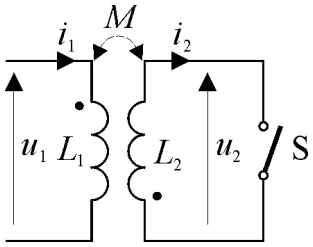

Fig. 4. Diagram – the principle of operation of a tunable inductive filter

The determination of a value of the equivalent inductance of the filter is based on the following analysis, using the basic properties of magnetically coupled circuits. The initial assumptions made do not take into account the nonlinearity of the (homogeneous) ferromagnetic core on which both coils are wound. The basic formulas (for sinusoidal variable excitation and for assumed zero resistance of both coils) describing the voltage and current relations in the circuit shown in Fig. 4 are as follows

$$U_1 = \mathrm{j}X_1 I_1 + \mathrm{j}X_{\mathrm{M}} I_2, \tag{8}$$

$$U_2 = \mathrm{j}X_2 I_2 + \mathrm{j}X_{\mathrm{M}} I_1, \tag{9}$$

where: X_1, X_2, X_{M} – respectively, own reactance of the coils and their mutual reactance.

As a result of transformations of (8) and (9), the following formula was obtained, describing the equivalent reactance of the filter

$$\mathrm{j}X_{\mathrm{TI}} = \frac{U_1}{I_1} = \mathrm{j}\left(X_1 - \frac{X_{\mathrm{M}}^2}{X_2}\right). \tag{10}$$

Considering (10) and the assumptions made, the mutual reactance of the coils (for the magnetic coupling of k) is determined by the formula

$$X_{\mathrm{M}} = k\sqrt{X_1 X_2}\Big|_{0 \le k \le 1}. \tag{11}$$

Assuming $X_1 = X_2 = X$, the final equation was obtained, making the value of the filter equivalent reactance dependent on the coupling factor k

$$X_{\mathrm{TI}} = \left(1 - S_{\mathrm{T\text{–}TI}} k^2\right) X\Big|_{S_{\mathrm{T\text{–}TI}}=0 \vee S_{\mathrm{T\text{–}TI}}=1}, \tag{12}$$

where: $S_{\mathrm{T\text{–}TI}} = 0$ – switch is in open state, $S_{\mathrm{T\text{–}TI}} = 1$ – switch is in closed state.

An example of the tunable filter implementation is shown in Fig. 5.

The main role is played by a two-winding transformer, (with a magnetic coupling coefficient equal to k), with a split secondary winding, to which a fast rectifier bridge (RCT) is attached. The rectifier output is connected to the collector of the

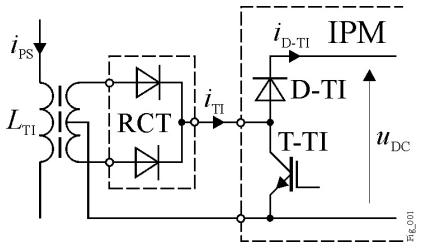

Fig. 5. Schematic diagram of the possible implementation of a tunable inductive filter

T–TI transistor (which acts as the S switch) and the "negative" rail of the DC circuit of the power supply. The shown filter configuration has an advantage which is the fact that the energy associated with the leakage flux (collected after the switch is closed) is transferred directly to the DC circuit of the power supply (after the switch is opened), which, taking into account the further assumed value of the k factor, clearly reduces power losses in the system.

It should be noted that in the above version of the filter, it is possible to achieve a smooth change of its so-called equivalent inductance – by changing a duty cycle of the control signal of the S switch (for example, in PWM mode). However, due to the step change of impedance seen through the secondary circuit of the system, it becomes nonlinear – Fig. 6. Considering the way of using the filter in the power supply, this nonlinearity has no significant (negative) impact on the effects of its operation.

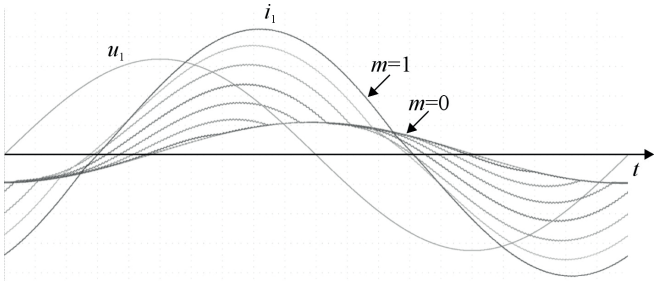

Fig. 6. Voltage and current waveforms at filter input, while the S key is controlled in the PWM mode and the modulation index varies in the range of 0.0–1.0, with its change equal to 0.1

In the 1-phase version of the power supply, the role of the branch with T–TI and D–TI elements can be played by the third branch of the IGBT module. These modules (especially in the IPM/IGBT version) are typically manufactured as 3-branch (i.e. 3-phase) [25]. This gives the proposed solution a clear economical value.

5. Control section

The block diagram of the power supply control section is shown in Fig. 7. In the current version of the power supply solution, it consists of, among others, two regulators and a filter's inductance control block:

- REGU – master voltage regulator in the DC circuit of the power supply, with a reference signal $U_{\mathrm{ref,U}}$ that controls the value of the amplitude of the (sinusoidal) reference signal $(u_{\mathrm{ref,I}})$ for the secondary grid current regulator; the controller output signal (u_{REGU}) is a step function (i.e. having a constant value) in the half-period of the reference signal $u_{\mathrm{ref,L}} = \sin(\omega_{\mathrm{L}} t)$,
- LIMU – limiter of the voltage regulator output signal magnitude, imposing the maximum value of the current at the input of the current source – in the context of the catalog parameters (i.e. current limitations) of the real IGBT switches,
- REGI –slave grid current regulator, based on a reference signal $u_{\mathrm{ref,I}} = u_{\mathrm{REGU}} u_{\mathrm{ref,L}}$, phase synchronized (via reference signal $u_{\mathrm{ref,L}}$) with both the grid voltage and feedback signal $u_{\mathrm{fb}} = r_{\mathrm{CT}} i_{\mathrm{L}}$, where r_{CT} is the transfer factor of the current transducer (CT),
- LIMI – limiter of the current regulator output signal magnitude, protecting the PWM block against over-modulation,
- PWM – signal generator,
- TIC – filter inductance control block.

The elements of the TIC are: ABS block, determining the absolute value of the REGU output voltage, summing node, comparing the voltage of this regulator with the reference voltage for the TIC block, and the comparator with the so-called dynamic hysteresis loop (DHC) [26], whose structure is shown in Fig. 8.

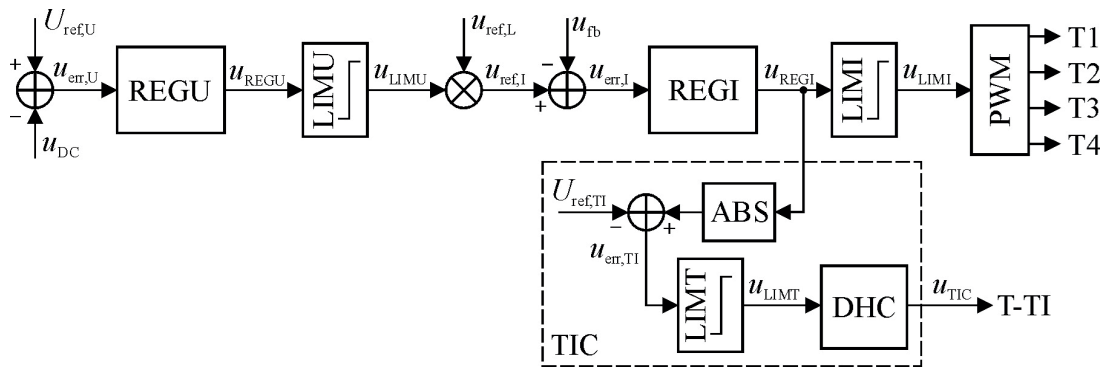

Fig. 7. The block diagram of the power supply control system

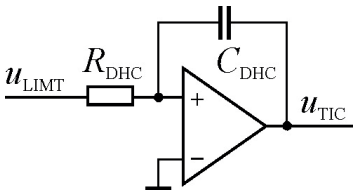

Fig. 8. Diagram of a comparator with dynamic hysteresis loop

The comparator operates on the signal $u_{\mathrm{err,TI}} = u_{\mathrm{REGI}} - U_{\mathrm{ref,TI}}$. If $u_{\mathrm{err,TI}} > 0$, the comparator output goes to a high state and the T–TI is switched on.

A comparator of this type (as opposed to a static comparator) provides a certain minimum pulse duration at its output – related to, among others, with its time constant $\tau_{\mathrm{DHC}} = R_{\mathrm{DHC}}C_{\mathrm{DHC}}$. As a consequence, also limiting to a pre-set maximum value, the frequency of such pulses – generated in a series. This feature is important for proper control of the T–TI switch – in terms of not exceeding its dynamical limitation. It results in both reducing power losses in the T–TI and the control system's resistance to electromagnetic disturbances. This feature was the main reason for choosing such a structure of the tunable filter control system. Because the comparator is a nonlinear and time-variant element, the relationship of width of its output pulse with the magnitude (and shape) of the input signal is only possible at a high level of generality. However, assuming the most extreme case of the dynamics of signal changes at the comparator input (i.e. a rectangular signal) and the magnitude of this signal being equal to the magnitude of the comparator output signal (which can be easily done by including a signal amplitude limiter at its input – here, the LIMT block), it can be shown [27] that in this situation, the comparator output pulse width will be smallest and equal to

$$\tau_{\mathrm{DHC,min}} = \left|\ln\frac{1}{3}\right| R_{\mathrm{DHC}}C_{\mathrm{DHC}} \cong 1.1 R_{\mathrm{DHC}}C_{\mathrm{DHC}}\,. \tag{13}$$

Due to the required time resolution of the output signal of the TIC block (except for the ABS block), it should have an analog implementation.

6. Linear model of power electronics current source

The linear model of the current source was developed to analyze its asymptotic stability as a closed automatic control system [28, 29]. The block diagram of the model is shown in Fig. 9. It consists of the following blocks: sample-and-hold amplifier

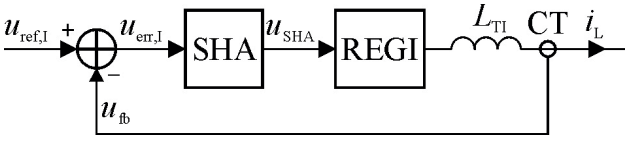

Fig. 9. Block diagram of the linear model of the power electronics current source

(SHA), current regulator (REGI), inductive filter, and current transducer (CT).

"Equivalent transmittance" of this model (discussed later) – SISO and LTV electrical system – is given by the following formula

$$G_{\mathrm{CS}}(\mathrm{j}\omega) = \frac{I_{\mathrm{L}}(\mathrm{j}\omega)}{U_{\mathrm{ref,I}}(\mathrm{j}\omega)} = \frac{K(\mathrm{j}\omega)}{1 + r_{\mathrm{CT}}K(\mathrm{j}\omega)}\,, \tag{14}$$

where:

$$K(\mathrm{j}\omega) = \frac{1}{\mathrm{j}\omega L_{\mathrm{TI}}} K_{\mathrm{SHA}}(\mathrm{j}\omega)K_{\mathrm{REGI}}(\mathrm{j}\omega), \tag{15}$$

where: $K_{\mathrm{SHA}}(\mathrm{j}\omega)$ is "transfer function" of the SHA block, $K_{\mathrm{REGI}}(\mathrm{j}\omega)$ is transfer function of current regulator, and $L_{\mathrm{TI}} = f(u_{\mathrm{err,TI}}, t) = \mathrm{var}$.

The SHA block, typically implemented as a ZOH (ZOH – Zero Order Hold), is a time-variant electrical system because the relationship between the output and input signals depends on the selection of sampling time, so it is a function of time [30, 31]. Therefore, one of the important formal conditions – in the classical approach – of the existence of its transmittance function is not met here. In further considerations, the so-called "equivalent transmittance" of the SHA block is used. This block operates only the static (stationary) part of (16) – binding the input and output signals of this block

$$\mathsf{F}\{u_{\mathrm{SHA}}\} = \mathrm{Sa}\left(\omega\frac{T_{\mathrm{S}}}{2}\right)\mathrm{e}^{-\mathrm{j}\omega\frac{T_{\mathrm{S}}}{2}} \sum_{n=-\infty}^{\infty} u_{\mathrm{err,TI}}(nT_{\mathrm{S}})\mathrm{e}^{-\mathrm{j}\omega nT_{\mathrm{S}}}, \tag{16}$$

where: T_{S} is signal sampling period, $\mathrm{Sa}(x) = \dfrac{\sin(x)}{x}$.

The LTV system generally significantly increases the complexity of the control algorithm [28, 29] because it requires consideration of the change in values of parameters of a particular object over time. Due to the possible, significant dynamics of changes in the value of current drawn by other nonlinear loads (NL), such a system is difficult to control by conventional methods (i.e. using conventional controllers). However, by assuming a certain, fixed value of the filter inductance and the fact that the current regulator is a P-type (with a DC gain of $k_{\mathrm{REGI,0}}$), the transmittance of the model takes the following form

$$K(\mathrm{j}\omega) = \frac{k_{\mathrm{REGI,0}}}{\mathrm{j}\omega L_{\mathrm{TI}}}\mathrm{Sa}\left(\omega\frac{T_{\mathrm{S}}}{2}\right)\mathrm{e}^{-\mathrm{j}\omega\frac{T_{\mathrm{S}}}{2}}. \tag{17}$$

Based on [32], to ensure system stability, the gain value must satisfy the following inequality

$$k_{\mathrm{REGI,0}} < 2\frac{L_{\mathrm{TI}}}{T_{\mathrm{S}}}\,. \tag{18}$$

For determination of (18), the effect of the aliasing phenomenon, characteristic for discrete-time systems, on the stability of the model was also considered. The formula (17) does not take into account filter resistance and grid impedance. However, for typical values of these quantities, their influence on the permissible gain value of the controller is negligible, while the complexity of (17) and (18) clearly increases.

7. Research on the system simulation model

In order to confirm the correctness of the initial assumptions of the system, its simulation model was built (in OrCAD/PSPICE environment), and the values of its basic parameters were as follows:

- nominal output power of power supply: 3.5 kVA,
- grid voltage parameters: 230 V/50 Hz,
- nominal input current (RMS value) of power supply: 15 A,
- maximal input current of power supply: 30 A,
- nominal output voltage of the power supply and the setting of its value range: 450 V $\pm$ 20%,
- tunable filter inductance: 5.0/1.4 mH ($k = 0.85$),
- sampling frequency in voltage and current regulators: 20 kHz,
- PWM carrier frequency: 10 kHz,
- reference signal (DC) for the TIC block: 310 V.

Fig. 10 shows selected test results for this model in the form of characteristic voltage and current waveforms – in operating conditions of power supply close to the nominal. They apply to a nonlinear (NL) load in the form of a thyristor voltage regulator with a firing angle of 90°, loaded with a resistor. Such a load, generating almost a step change in the network current, with a significant amplitude value, imposes extremely high requirements on the desired dynamics of input current changes (i_{PS}). Thus, it is well suited for analyzing the quality of the proposed converter's operation.

As the basic quantities, characterizing the quality of the i_L current, both *TTHD* and the duration of the transient state (τ_L) – after a step change in the value of the nonlinear load current – were chosen. The *TTHD* coefficient was calculated on the basis of an RMS value of the current and the value of its basic harmonic.

As a result of testing the simulation model, the following values of these quantities were obtained:

- compensation function off: $TTHD = 12.9\%$,
- compensation function on and constant value of inductance of filter: $TTHD = 5.15\%$, $\tau_L = 0.6$ ms,
- compensation function on and tunable value of inductance of filter: $TTHD = 2.10\%$, $\tau_L = 0.2$ ms.

The obtained results show a clear, i.e. approx. 2.5-times, according to *TTHD*, and 3-times, according to τ_L, improvement in current quality, as a result of a PS with tunable inductance operating.

Fig. 11, in turn, presents details of waveforms, related to the operation of the tunable filter in the transient state of the nonlinear load current, caused by the thyristor switching on. These are shown for three different DHC time constants, equal to: 10, 5, and 2 μs.

As expected, as the time constant of the comparator decreases, the impulses at its output narrow and its number in the series increases, and therefore the transient impulse component in the source current decreases – at the expense of the increase in dynamic losses in the T–TI and D–TI elements (however, these power losses were not estimated in the work). At the same time, the duration of the transient state in the source and grid current remains unchanged. The filter control process is therefore scalable in time, and the results of its operation are predictable.

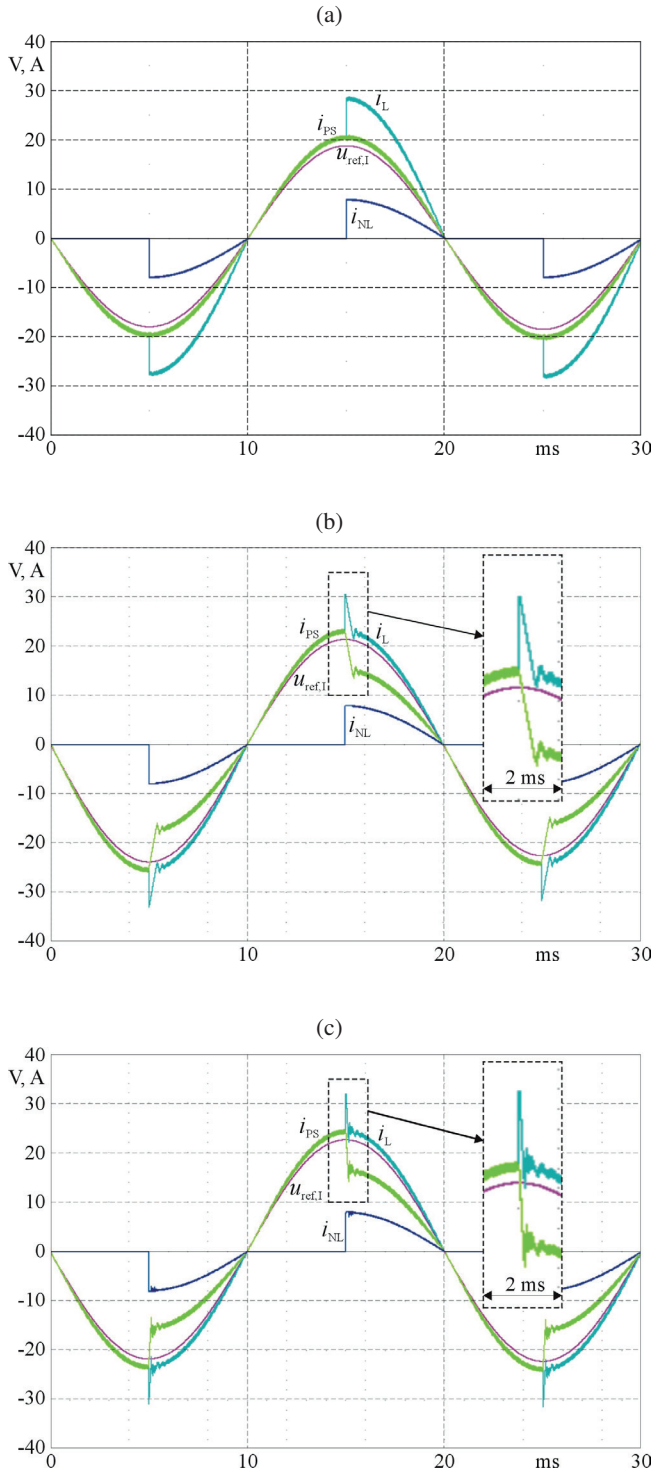

Fig. 10. Grid voltage and current waveforms in a system simulation model: a) with the reactive and distortion power compensation function turned off, b) with the compensation function turned on and constant inductance filter, and c) with the compensation function turned on and the tunable inductance filter

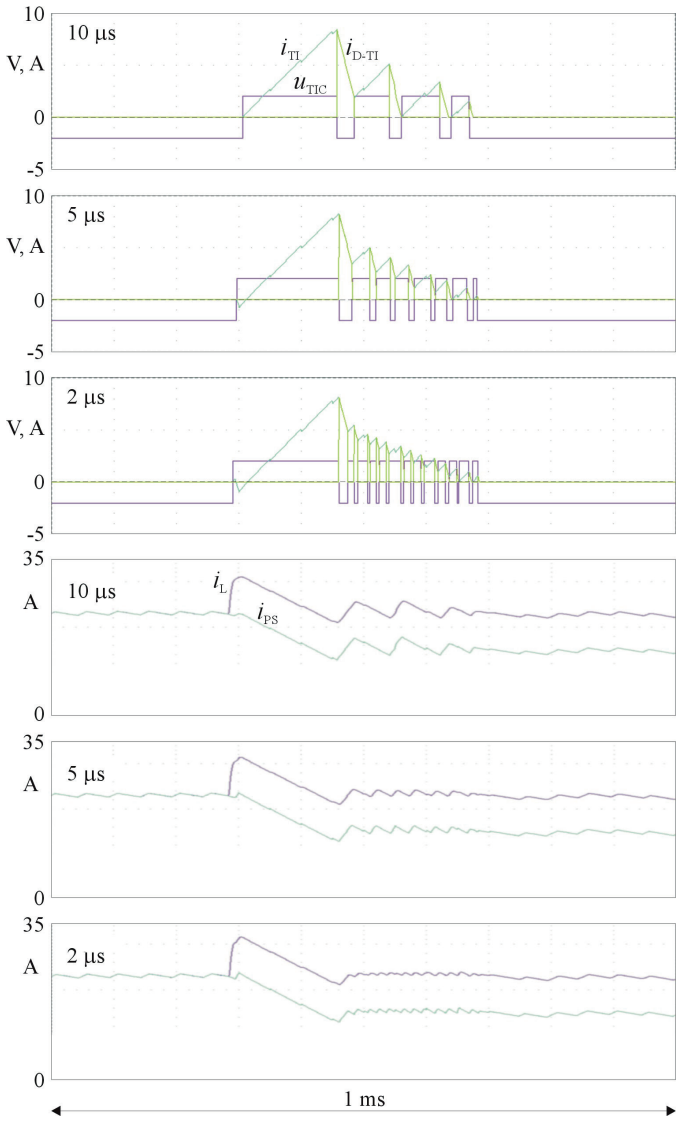

Fig. 11. Details of signal waveforms in the transient state of a nonlinear load current – for three different time constants of a comparator (DHC). The upper part of the figure: comparator output signal (red), filter secondary current (blue), and D–TI diode current (green). The lower part of the figure: grid current (red) and input current of the current source (blue)

8. Summary

The subject of the work was confirmation of the correct operation of the power electronics converter with a tunable inductive filter at the input, acting as a power supply with the function of parallel active compensation of reactive and distortion power. These powers were generated by external nonlinear loads, connected to the same power grid node as the power supply.

The use of a tunable inductive filter allowed to significantly increase the dynamics of current changes at the power supply input – in relation to a system with a constant value of this inductance. The results of the tests of the system simulation model indicate a clear (2.5- and 3-times, according to the indicators specified in the work) improvement in the quality of the system operation when a tunable inductance filter is used.

The proposed algorithms for controlling the system can more effectively improve the quality of the power grid voltage – compared to classical solutions with PFC. At the same time, thanks to the relatively small degree of increase in the hardware complexity of the power supply (compared to the version without compensation function), it can be an economically attractive alternative to typical (i.e. functionally specialized) active parallel filters.

References

[1] B. Kroposki, C. Pink, R. DeBlasio, T. Holly, M. Simöes, and K.S. Pankaj, "Benefits of power electronic interfaces for distributed energy systems", *IEEE Trans. Energy Convers*. 25, 901–908 (2010).

[2] R.L. Kirlin, C. Lascu, and A.M. Trzynadlowski, "Shaping the noise spectrum in power electronic converters", *IEEE Trans. Ind. Electron*. 58, 2780–2788 (2011).

[3] A. Benchabira and M. Khiat, "A hybrid method for the optimal reactive power dispatch and the control of voltages in an electrical energy network", *Archives of Electrical Engineering* 68, 535–551 (2019).

[4] L.S.M. Depenbrock, D.A. Marshall, and J.D. Van Wyk, "Formulating requirements for a universally applicable power theory as control algorithm in power compensators", *Eur. Trans. Electr. Power* 4 (6), 445–455 (1994).

[5] M. Pasko, D. Buła, K. Dębowski, D. Grabowski, and M. Maciążek, "Selected methods for improving operating conditions of three-phase systems working in the presence of current and voltage deformation – part I", *Archives of Electrical Engineering* 67 (3), 591–602 (2018).

[6] M. Siwczyński and M. Jaraczewski, "Reactive compensator synthesis in time-domain", *Bull. Pol. Ac.: Tech*. 60 (1), 119–124 (2012).

[7] K. Mikołajuk and A. Toboła, "Average time–varying models of active power filters", *Przegląd Elektrotechniczny* 95 (1), 53–55 (2010).

[8] H. Akagi, E.H. Watanabe, and M. Aredes, *Instantaneous power theory and applications to power conditioning*, John Wiley & Sons Inc., Published by John Wiley & Sons, New Jersey, ISBN: 978-0-470-10761-4, 2007.

[9] K.K. Shyu, M.J. Yang, C.Y.M Chen, and Y.F. Lin, "Model reference adaptive control design for a shunt active-power-filter system", *IEEE Trans. Ind. Electron*. 55, 97–106 (2008).

[10] A. Kouzou, M.O. Mahmoudi, and M.S. Boucherit, "Evaluation of the Shunt Active Power Filter apparent power ratio using particle swarm optimization", *Archives of Control Sciences* 20, 47–76 (2010).

[11] A. Szromba, "Shunt power electronic buffer as active filter and energy flow controller", *Archives of Control Sciences* 62, 55–75 (2013).

[12] M. Gwóźdź, "Power electronics active shunt filter with controlled dynamics", *COMPEL: The International Journal for Computation and Mathematics in Electrical and Electronic Engineering* 32 (4), 1337–1344 (2013).

[13] K. Antoniewicz and K. Rafal, "Model predictive current control method for four-leg three-level converter operating as shunt active power filter and grid connected inverter", *Bull. Pol. Ac.: Tech.* 65 (5), 601–607 (2017).

[14] W. Śleszyński, A. Cichowski, and P. Mysiak, "Current harmonic controller in multiple reference frames for series active power filter integrated with 18-pulse diode rectifier", *Bull. Pol. Ac.: Tech.* 66 (5), 699–704 (2018).

[15] M. Maciążek and D. Grabowski, "Comparison of active power filter control algorithms", *Prace Naukowe Politechniki Śląskiej. Elektryka*, Silesian University of Technology 4 (236), 7–17 (2015) [in Polish].

[16] L. Huber, Y. Jang, and M.M. Jovanovic, "Performance evaluation of bridgeless PFC boost rectifiers", *IEEE Trans. Power Electron*. 23, 1381–1390 (2008).

[17] A. Bogdan, "Modeling of the AC/HF/DC converter with power factor correction", *Archives of Electrical Engineering* 59, 141–152 (2010).

[18] M. Mahdavi and H. Farzanehfard, "Bridgeless SEPIC PFC rectifier with reduced components and conduction losses", *IEEE Trans. Ind. Electron*. 58, 4153–4160 (2010).

[19] X. Xie, C. Zhao, L. Zheng, and S. Liu, "An improved buck PFC converter with high power factor", *IEEE Trans. Power Electron*. 28, 2277–2284 (2013).

[20] H. Choi, "Interleaved boundary conduction mode (BCM) buck power factor correction (PFC) converter", *IEEE Trans. Power Electron*. 28, 2629–2634 (2013).

[21] Y. Rozanov, S. Ryvkin, E. Chaplygin, and P. Voronin, *Fundamentals of power electronics: operating principles, design, formulas, and applications*, CRC Press, 2015.

[22] M.H. Rashid, *Power Electronics Handbook*, Elsevier Ltd. Oxford, ISBN: 0-12-581650-2, 2018.

[23] M. Krystkowiak, "Modified model of wideband power electronics controlled current source with output current modulation", *Elektronika – konstrukcje, technologie, zastosowania* 57 (11), 65–70 (2016) [in Polish].

[24] W. Kester, *The Data Conversion Handbook*, Analog Devices Inc, Newnes, 2005.

[25] Mitsubishi Electric, Intelligent Power Modules. http://www.mitsubishielectric.com/semiconductors/products/powermod/intelligentpmod/index.html. Accessed: August 2019.

[26] M. Gwóźdź, "Broadband power electronics controlled voltage source with output stage based on GaN transistors", *Przegląd Elektrotechniczny* 95 (5), 70–73 (2018).

[27] M. Gwóźdź, "Power electronics programmable voltage source with gan modules in power stage", *Proceedings of the XIV National Conference Control in Power Electronics and Electric Drives SENE 2019*, Łódź, November 20-22 (2019).

[28] T. Kaczorek, *Fundamentals of control theory*, Edition II, Scientific and Technical Publishing House, Warsaw, 2005, 2006 [in Polish].

[29] J.C. Doyle, B.A. Francis, and A.R. Tannenbaum, *Feedback Control Theory*, Dover Publications, ISBN: 130632548X, 2013.

[30] B. Francis and T. Georgiou, "Stability theory for linear time-invariant plant with periodic digital controllers", *IEEE Trans. Autom. Control* 33 (9), 820–832 (1988).

[31] L. Mirkin, "Transfer functions of sampled-data systems in the lifted domain", in *Proc. 44th IEEE Conf. on Decision and Control & European Control Conf. ECC'05* (Seville, Spain), 5180–5185 (2005).

[32] M. Gwóźdź, "Stability of discrete time systems on base of generalized sampling expansion", *Prace Naukowe Politechniki Śląskiej. Elektryka*, Silesian University of Technology 1 (217), 29–40 (2011).